Crystallization and Pressure Filtration of Anhydrous Milk Fat: Mixing Effects

D.B. Patience[a], R.W. Hartel[a,*], and D. Illingworth[b]

[a]Department of Food Science, University of Wisconsin, Madison, Wisconsin 53706, and
[b]New Zealand Dairy Research Institute, Palmerston North, New Zealand

ABSTRACT: Melt crystallization of anhydrous milk fat and subsequent filtration of the slurry is a common process for obtaining milk fat fractions with different physical and chemical properties. The crystallization mechanism is very complex and little is known about how the crystallizer conditions and the crystal size distribution (CSD) affect the filtration process. The objective of this study was to characterize the fractionation process and determine which geometric parameters of the crystallizer affect the filtration step. Two scales of fractionation were studied, 0.6 L and 3.6 L, with crystallization at 28°C. The slurry was pressure-filtered after 24 h at 500 kPa in a 1-L chamber. Impeller diameters and speeds were varied for both scales. Photomicroscopy and spectrophotometry were used to characterize the crystallization process, and filtration rates were measured by weighing the amount of filtrate passing through the filter. Filtration resistance values, calculated using the constant pressure filtration equation, as well as photomicroscopy results indicated that the agglomerates and crystals that formed had different morphological characteristics for the different mixing and flow regimes in the crystallizer. Crystallization conditions that provide an optimal filtration time, a solid fraction with minimal liquid entrainment, and a CSD with an intermediate range of sizes (80–500 μm) having good packing properties for filtration were found.

Paper no. J9087 in *JAOCS 76*, 585–594 (1999).

KEY WORDS: Crystallization, filtration, fractionation, milk fat, pressure.

Milk fat has a unique composition, consisting of 98% (w/w) triacylglycerols with fatty acids ranging in length from C_4 to C_{18} (1). Its wide melting range makes it unsuitable for use in many applications, but it is this same wide range that makes milk fat an ideal raw material for production of specialty ingredients. The chemical and physical properties of milk fat can be altered by many techniques such as hydrogenation, enzymatic modification, chemical interesterification, and fractionation. Milk fat has been fractionated by supercritical carbon dioxide extraction (2–5), molecular distillation (6), or crystallization either from the melt (7–9) or a solvent (10,11). When crystallized, the resultant slurry is filtered by either vacuum filtration (11–15), pressure filtration (16–18) or filter centrifugation (19,20) to produce fractions with various chemical compositions and physical attributes.

Milk fat fractions may be used as ingredients in a wide range of products. For example, fractionation is commonly used in improving the spreadability of butter (21). Milk fat fractions can be combined with other milk fat fractions or anhydrous milk fat (AMF) to produce butters with improved spreadability at standard refrigerator temperatures (5°C). High-melting milk fat fractions may be used in chocolate to enhance flavor, reduce costs, soften the chocolate, and inhibit fat bloom (21–25). Hard milk fat fractions produced from dry fractionation also have been shown to be excellent for puff pastries, imparting a desirable butter flavor (12).

Crystallization from the melt, or dry fractionation, is the technique most commonly employed to fractionate milk fat. Deffense (18) discussed four factors that influence crystallization of milk fat: oil composition, intersolubility, polymorphism, and the technique of crystallization. The complex composition of milk fat complicates the crystallization process. Because milk fat has more than 40 different fatty acids, a wide range of different triacylglycerols is present and these may change with the season. Grall and Hartel (9) crystallized milk fat sequentially to final temperatures of 30, 20, and 15°C, in experiments where the crystals were separated by vacuum filtration and then the liquid was cooled to the next temperature. Crystals formed at 30°C consisted of conglomerates of needle-like structures, whereas those that formed at 20°C consisted of smaller, tighter conglomerates of plate-like structure. The crystals from the 15°C fractions formed uniform spheres with a single birefringent cross in polarized light, suggesting a mixed structure of crystalline and liquid regions.

The techniques used to crystallize milk fat (the type of crystallizer and operating conditions) can significantly affect the crystallization process. Deffense (12) studied the influence of cooling rate on crystallization of milk fat. A fast cooling rate induced the formation of many nuclei early in the crystallization process and these nuclei remained through the crystallization run. Large milk fat agglomerates formed, leading to a poor product yield and quality. A slow rate of cooling led to the formation of regular milk fat crystals that were

*To whom correspondence should be addressed at Department of Food Science, University of Wisconsin, 1605 Linden Dr., Madison, WI 53706.
E-mail: hartel@calshp.cals.wisc.edu

easily filtered, producing a consistent product yield and quality.

Black (15) studied parameters affecting milk fat crystallization and filtration of the milk fat slurry. The variables found to influence crystallization most significantly were the precooling treatment (removal of crystal memory or not), the cooling method (programmed or exponential), the cooling time (short or long), and the agitator speed (10 or 20 rpm). The best conditions were preheating of the milk fat to remove crystal memory, then a programmed linear cooling rate of the cooling water, and a crystallization time of 8 h with slow agitation (10 rpm). These conditions resulted in rapid filtration (13.2 $kg \cdot min^{-1} \cdot m^{-2}$), fractions with minimum solid yield (31.4%), and an intermediate mean crystal size (308 μm).

Liquid entrainment within the solid fraction after filtration influences the physical and chemical quality of the desired fraction in commercial processes. Entrainment of more liquid-like components of milk fat can arise for two reasons: (i) formation of mixed crystals in the form of agglomerated spherulites that adsorb liquid within the crystal or (ii) liquid oil remaining between individual spherulite crystals in the filtration bed. During formation of agglomerated crystals, liquid oil adsorbed to the individual needles remains within the spherulitic, agglomerated crystalline structure. This liquid entrainment is often worst during rapid crystallization when mixed crystals of widely diverse triacylglycerol structure are formed. Liquid entrainment within the filtration bed is dependent on the number, size, shape, and chemical composition of the crystals, the method of crystallization, and the method of filtration (11,26). Uniformly sized and shaped crystals filter well with minimal liquid entrained between crystals, whereas a crystal slurry with wide distribution of sizes has liquid trapped between crystals. The first mechanism of entrainment is influenced primarily by crystallization conditions, whereas the latter mechanism is influenced by filtration characteristics.

Despite the many studies on melt crystallization of AMF (26), little work has been reported relating the processing conditions of crystallization with subsequent filtration of the crystal slurry. The objectives of this research were to characterize the melt fractionation process of AMF and determine which geometric parameters of the crystallizer affect the filtration process.

MATERIALS AND METHODS

AMF was obtained from a local dairy in three 40-lb (18-kg) pails. The milk fat was melted and then filtered through Whatman #1 filter paper (Retention "medium crystalline", Whatman International Limited, Maidstone, England) to remove any particulate impurities. Nonuniformity in composition between batches was eliminated by storing 3.4-kg milk fat samples in sixteen 1-gal (3.8-L) high-density polyethylene containers (Airlite, Omaha, NE) using blended milk fat from all three storage pails. The milk fat was then stored at 5°C until used.

AMF was crystallized in one of two jacketed, round-bottomed, stainless steel tempering beakers (Cole Palmer Instrument Company, Chicago, IL) of 0.6 or 3.6 L volume. The crystallizers were geometrically similar, with H/T_{ID} ratios (liquid level height/tank inside diameter) constant at 0.8. For the 3.6 L crystallizer, 3.2 kg of milk fat was used. The H from the center of the large crystallizer was 148 mm (5.84″). For the 0.6 L crystallizer, 0.65 kg of milk fat was used. The amount of fat removed during sampling was taken into account so the average volume of the 0.6 L crystallizer was geometrically similar to the 3.6 L crystallizer. The average liquid level height for the 0.6 L crystallizer was 79 mm (3.12″).

A staggered arrangement of three propellers was used as the agitator (impeller) for all of the experiments. The agitator shaft was centered using a centerboard. The bottom clearance ratio (C_1/D) was kept constant for all experiments at a value of 0.2. The agitator shaft had measured notches on it for the different propeller sizes, and the propellers were aligned with the top of the centerboard to keep the respective (C_1/D) ratio constant at 0.2. The top clearance ratio (C_4/D) of the top propeller from the liquid surface was also 0.2. For the small-scale crystallizer, the top clearance ratio was based on the average liquid level height of 79 mm. The agitator speed was controlled manually using a Master Servodyne Controller and Drive unit (Model 4445-30; Cole Palmer Instrument Company).

The temperature of the cooling water was controlled and circulated through the jacket of the beaker using a constant temperature water bath (VWR Model 1157; VWR Scientific Company, Niles, IL). The available heat flux was calculated as 195 $kW \cdot m^{-2}$ for both scales of crystallization. The flow rate of water through the crystallizers was measured using a flow meter (Gilmont Instruments, Niles, IL) and controlled at 2.7 and 6.3 $L \cdot min^{-1}$ for the 0.6 and 3.6-L crystallizers, respectively. The residence time for cooling water through the water jackets of both crystallizers was 6 s.

The milk fat was held at 60°C for 1 h to remove any possible crystal memory. The final crystallization temperature was achieved by cooling the water bath to 28°C. The water bath cooled exponentially to the final crystallizing temperature, thus cooling the milk fat exponentially.

A duplicated 3×3 randomized block design (27) was used to study the influence of agitator diameter or D/T_{ID} ratio) and agitator speed in the 0.6-L crystallizer. Propeller diameters (D) were 38 (1.5″), 51 (2.0″), and 76 mm (3.0″), which gave D/T_{ID} ratios of 0.38, 0.51, and 0.77, respectively. All other geometric shape factors were constant for all experiments. The levels of agitator speed (N) were 50, 100 and 150 rpm. The tip speed was calculated using Equation 1 (28) to combine agitator diameter and speed into one parameter that described mixing in the crystallizer.

$$u_{tip} = \pi ND \quad [1]$$

where u_{tip} is the tip speed, tangential to the agitator at the edge of the agitator, N the agitator rotational speed, and D the agitator diameter.

To compare data over geometrically similar scales, Equation 1 was scaled by dividing tip speed by the inside diameter (T_{ID}) of the tank to get Equation 2. This is a scaled tip speed (u_{scaled}),

$$u_{scaled} = \pi N(D/T_{ID}) \quad [2]$$

A duplicated experiment using the 76-mm (3.0″) triple propeller arrangement in the small-scale crystallizer at a rotational speed of 12.5 rpm was done to study the slowly agitated laminar mixing regime. The 76-mm (3.0″) triple propeller arrangement at rotational speeds of 40, 95, and 160 rpm was also studied in the 3.6-L crystallizer in another set of duplicated experiments. The 3.6-L crystallizer was geometrically similar to the 0.6-L crystallizer, excluding the (D/T_{ID}) shape factor.

After 24 h of crystallization, the milk fat slurry was pressure-filtered. The contents of the 0.6-L crystallizer were poured into the benchtop pressure filter (New Zealand Dairy Research Institute, Palmerston North, New Zealand) and filtered at one time. For the 3.6-L crystallizer, two 0.5-L batches of the slurry from one experiment were filtered. The main dimensions and design of the filter are shown in a simplified engineering drawing for a 1-L pressure filtration apparatus (all dimensions in mm; cw, cold water; not to scale) (Scheme 1). The pressure filter was held at the same temperature as the crystallizer by circulating water from the bath. It was assumed that no further crystallization took place within the vessel once it was loaded with the milk fat slurry. All pressure filtration experiments were performed at 500 kPa (72.5 psig). The slurry was filtered through two sheets of Whatman #1 filter paper (Retention "medium crystalline", Whatman Interna-

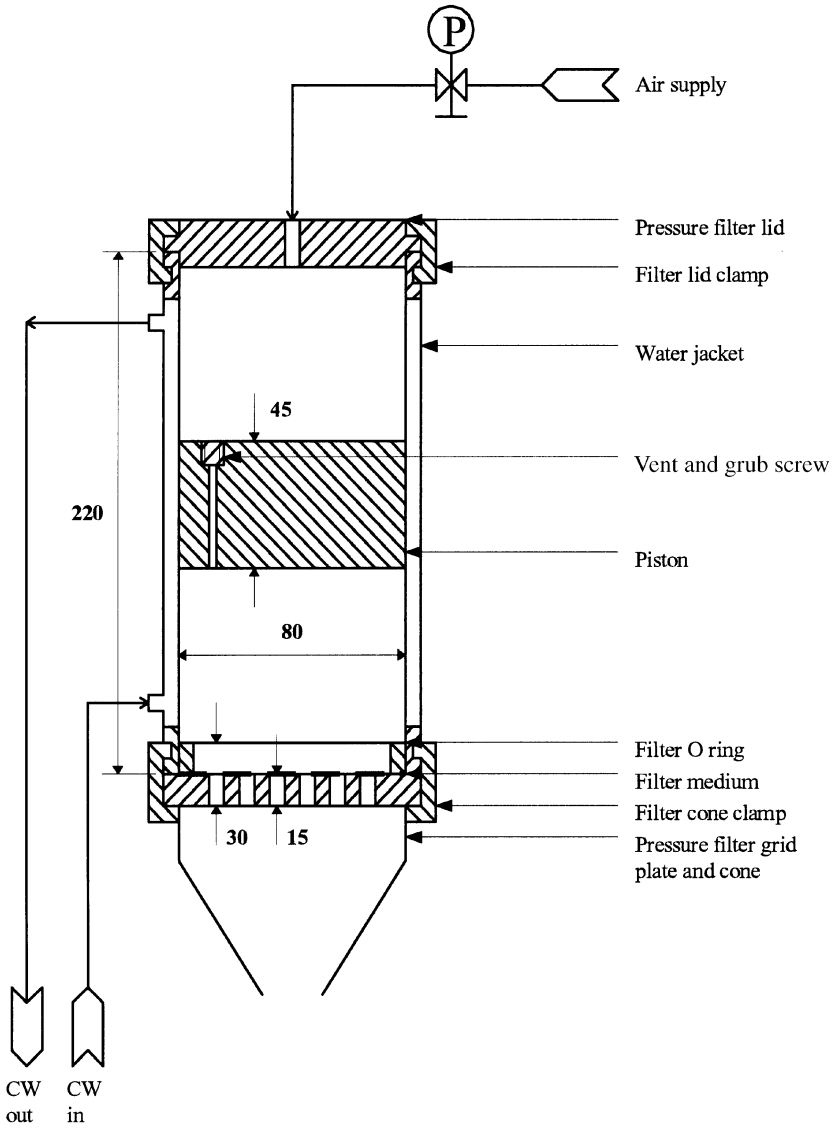

SCHEME 1

tional Limited). The mass of filtrate draining from the filter was measured by using a scale situated beneath the filter.

Crystal growth kinetics for each crystallization experiment were measured as change in geometric mean size of the crystal size distribution and as decrease in transmittance using a spectrophotometer. A Nikon [Optiphot, Nippon Kogaku (USA) Inc., Garden City, NY] microscope equipped with a 35-mm camera was used to take photomicrographs of milk fat crystal slurries. In addition, transmittance readings (Spectronic 20 spectrophotometer, Bausch and Lomb, Rochester, NY) of the milk fat were recorded every 15 min for the first hour of the experiment, and then every 5 to 10 min until the transmittance started to decrease at the onset of crystallization. Once the transmittance decreased, samples of the milk fat slurry were taken from the crystallizer for photomicroscopy. The microscope cell was fixed to a temperature plate held at the same temperature as the crystallizer.

All photomicrographs were taken under ordinary light at a magnification of 10×. The crystal size distribution was determined by image analysis of $3.5 \times 5''$ photomicrographs. The perimeter of each crystal was manually traced on a digitizer board (Model MM 1812, Summagraphics, Fairchild, CT) with the results being transferred to a microcomputer (IBM PS2 Model 30, International Business Machines Corporation, Boca Raton, FL). The projected area (mm^2) of each crystal was collected by image analysis software (Sigma Scan, Jandel Scientific, Sausalito, CA). An equivalent circular diameter was calculated from the traced particle area, assuming that the traced area was equivalent to a circle. The data were then arranged into a crystal size distribution, with intervals of size 50 μm, from 0 to 1000 μm. Each photomicrograph was used to generate a crystal size distribution at its respective crystallization time. Each crystal size distribution was analyzed individually. Arithmetic and geometric mean diameters, variances, standard errors and coefficients of variation were calculated for each distribution.

To determine crystal growth kinetics, the change in the geometric mean size of the fat crystal size distribution with time, $L'(t)$, was fitted to Equation 3.

$$L'(t) = L_s \left\{1 - \exp\left[-\frac{(t - L_D}{\tau_c}\right]\right\} \quad [3]$$

where L_s is the steady-state geometric mean crystal diameter, L_D is the lag time before crystallization occurred, and τ_c is the time constant associated with crystallization. Data for change in mean size with time were fitted to Equation 3 using multiple nonlinear regression to obtain the best-fit parameters.

The resistance to flow of filtrate around the crystals was quantified during the pressure filtration process. Filtration resistance of the milk fat crystals, which is dependent on crystal morphology and size distribution, was measured using the constant pressure filtration equation (28), given as Equation 4.

$$dt/dm = (\mu\alpha\omega/\rho^2A^2P)m + (\mu R_m/\rho AP) \quad [4]$$

where dt/dm is the reciprocal mass filtrate flow rate ($s \cdot kg^{-1}$), m the mass of filtrate (kg), μ the liquid viscosity [Pa·s], α the specific filter cake resistance ($m \cdot kg^{-1}$), ω the solids (crystal) concentration in slurry ($kg \cdot m^{-3}$), ρ the filtrate density ($kg \cdot m^{-3}$), A the filter cross-sectional area (m^2), P the applied gauge pressure or pressure drop (Pa), and R_m the filter medium resistance (m^{-1}). The term $\mu\alpha\omega/\rho^2A^2P$ can be treated as a single parameter and used as a filtration resistance instead of determining α, the specific filter cake resistance. Reciprocal mass flow rate was plotted against respective mass and the slope of the line determined using least squares to get the lumped filtration resistance ($s \cdot kg^{-2}$).

Filtration efficiency was determined by measuring the absorbance of colored compounds in milk fat, which consist mainly of carotenoids and similar compounds, called carotene (20). It was assumed that carotene did not cocrystallize with the milk fat crystal and remained entirely with the liquid fat. This assumption has been shown to be valid for solids content <35.0% (29). Thus, any color in the solid fraction after filtration was due to entrapped liquid. A simple mass balance of liquid and solid fractions allowed calculation of an efficiency of filtration, defined as the ratio of the difference in absorbance of the liquid (C_l) and solid fraction (C_s), compared with the absorbance of the original milk fat (C_o), Equation 5 (20):

$$\text{efficiency} = 100[(C_l - C_s)/C_o] \quad [5]$$

Evans (20) derived a formula from a mass balance for calculating the true solids concentration in the filter cake from the absorbance of carotene in the solid and liquid fractions, given in Equation 6.

$$\text{true solids fraction} = (m_s/m_o)[(C_l - C_s)/C_l] \quad [6]$$

where m_s/m_o is the solid fraction yield. Hence, entrainment is derived as in Equation 7,

$$\begin{aligned}\text{entrainment} &= 100[m_s - (m_o \times \text{true solids fraction})]/m_s \\ &= 100(C_s/C_l)\end{aligned} \quad [7]$$

The maximum absorbance of light, measured using a Spectronic 20 spectrophotometer, of carotene in milk fat was found to be at 460 nm. This wavelength was used for the filtration efficiency measurement. At the beginning of each crystallization experiment, the absorbance of light in the original milk fat at 60°C was measured in triplicate. After filtration, the solid fraction was melted at 60°C and the liquid fraction was heated to 60°C. Absorbance readings of the two samples were measured in triplicate and the efficiency calculated.

Melting points of milk fat and its fractions were measured using the capillary tube method (clear point) of the American Oil Chemists' Society (30). The melting point (or clear point) of the fraction was taken as the average of the three replicates at the point when each tube became completely clear upon slow melting.

RESULTS AND DISCUSSION

Morphology. The shape and size distribution of crystals varied with the operating conditions. For the conditions of slow agitation with scaled tip speed of 1.0 s^{-1}, many large, loosely bound agglomerates formed with some very small crystals below the measurable limit. The measurable size distribution range for crystals was 25 to 620 μm. Large agglomerates formed because of the poor heat transfer and slow agitation in the crystallizer. This allowed the agglomerates to collide more frequently with each other without being broken up by shear forces.

For the system with a scaled tip speed of 2.0 s^{-1}, fewer agglomerates formed. These agglomerates had a tightly packed structure consisting of what appeared to be uniform spherulitic milk fat crystals. Many uniform spherulites were also present individually in the melt solution. The size distribution range for crystals was 40 to 600 μm.

For the system with a scaled tip speed of 6.0 s^{-1}, many particles formed. Heat transfer in the crystallizer was rapid under these conditions, and many nuclei formed early in the crystallization process and grew quickly. However, owing to the high degree of agitation, many crystals were broken by the impeller and so the overall mean diameter remained small. The size distribution range for crystals was 25 to 300 μm.

Filtration kinetics. Figure 1 shows a typical filtration flow curve, fitted to the filtration resistance equation Equation 4. In section (a) of the graph, the milk fat slurry was compressed in the pressure filter. The crystals and agglomerates settled into a packing arrangement that formed the cake. In section (b), constant pressure filtration occurred and the remaining liquid flowed through the cake. The cake was assumed to be incompressible in this section, because the data resulted in a linear fit to Equation 4. The slope of this section was measured and used as the lumped filtration resistance in Equation 4. The lumped filtration resistance is related to the crystal size distribution and to crystal and agglomerate morphology. The final section of the filtration curve, section (c), was where filtration had effectively ended and only a few final drops of liquid exited the pressure filter.

Figure 2 shows a comparison of all the filtration resistances of the resultant slurries as a function of the operating conditions, in terms of the scaled tip speed, of the crystallizers. The error bars in Figure 2 are 90% confidence intervals. The wide error bars in some cases demonstrate the variability in filtration rates that arises when experimental conditions are repeated. That is, crystallization at the same conditions gave faster or slower filtration rates, most likely because of the somewhat uncontrolled nature of crystallization.

For the 0.6-L crystallizer, a minimum in filtration resistance occurred at a scaled tip speed of 2.0 s^{-1} (0.6-L crystallizer with the 76-mm propeller at an agitation speed of 50 rpm), which gave a filtration time of approximately 7 min. At these optimal operating conditions, a relatively uniform crystal size distribution formed which had good packing properties during filtration. There were few small crystals and many intermediate size crystals of range 50 to 400 μm. For the operating conditions at a scaled tip speed of 0.5 s^{-1} (0.6-L crystallizer with the 76-mm propeller at an agitation speed of 12.5 rpm), the slurry took approximately 16 min to filter. At this

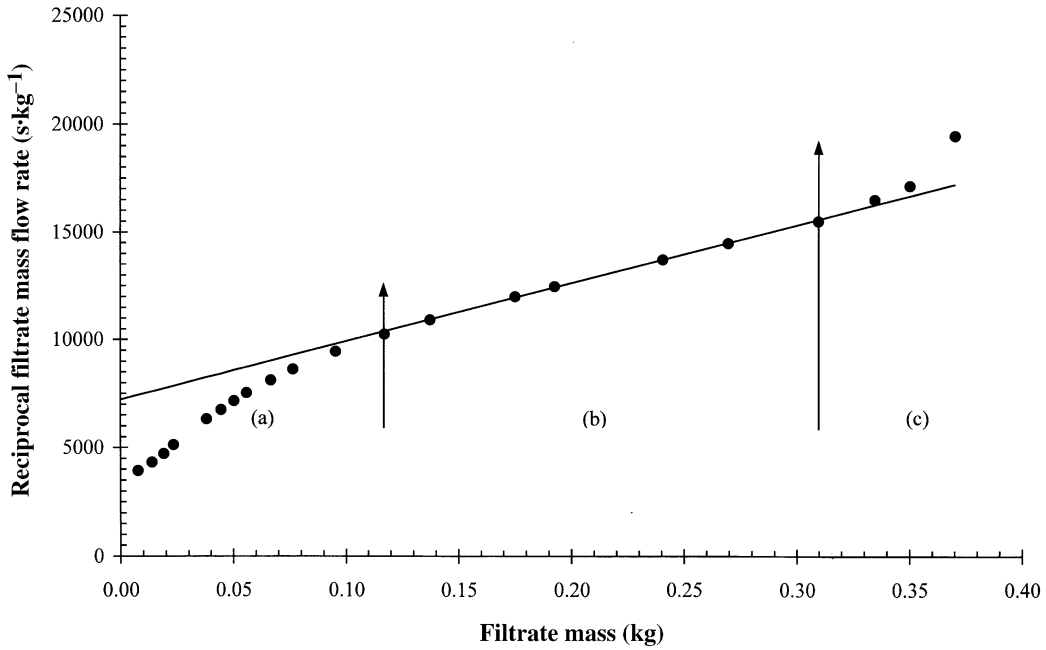

FIG. 1. Filtration flow curve of slurry after batch crystallization of anhydrous milk, showing the initial cake formation period (a), constant pressure filtration (b) described by Equation 4, and completion of filtration (c) (0.6 L, 76 mm, 100 rpm, 28°C, 200 kPa).

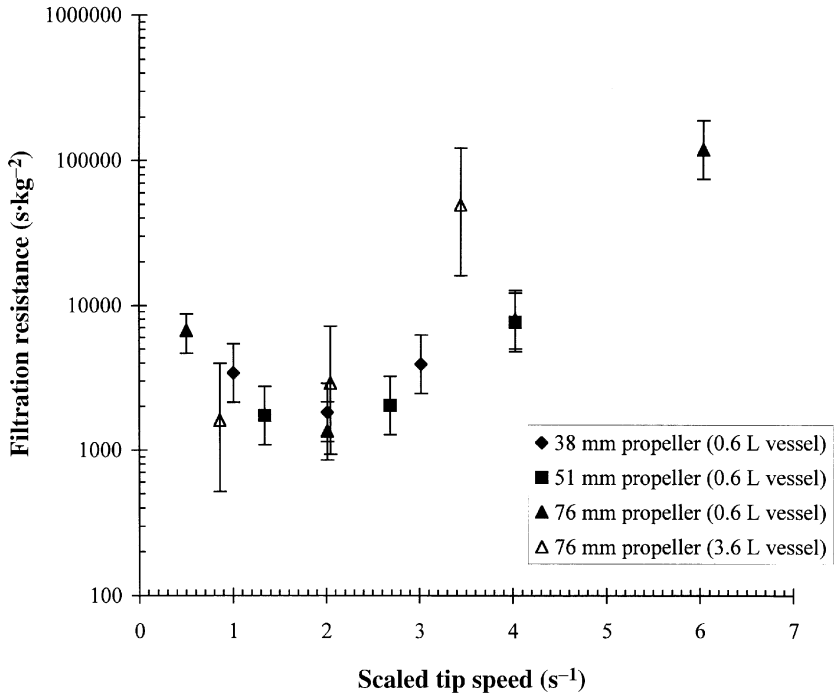

FIG. 2. Comparison of filtration resistances (Eq. 4) of resultant slurries from batch crystallization of anhydrous milk fat (0.6 L and 3.6 L, 28°C, 500 kPa). Error bars are 90% confidence intervals.

low agitation speed (12.5 rpm), the crystallizer operated under laminar mixing conditions. The milk fat crystals had little contact with the agitator and tended to collide more frequently with other milk fat crystals, agglomerating to form large particles. However, a significant number of very small crystals were also present. These small crystals plugged the gaps between large crystals and inhibited liquid flow during filtration. For the highly agitated conditions at a scaled tip speed of 6.0 s^{-1} (0.6-L crystallizer with the 76-mm propeller at an agitation speed of 150 rpm), the slurry took more than 1 h to filter. Crystallization under highly agitated conditions produced many small crystals of size 30 to 350 μm as a result of attrition. This type of slurry was very difficult to filter. The particles were very small with large surface area to particle volume ratio.

The experiments with the 3.6-L crystallizer produced filtration results that did not follow the trend of the 0.6-L crystallizer in terms of scaled tip speed. At a scaled tip speed of 2.0 s^{-1} (3.6-L crystallizer with the 76-mm propeller at an agitation speed of 40 rpm), the slurry took, on average, 11 min to filter. A possible reason for the difference in filtration results may be that the crystals in the 3.6-L crystallizer have a smaller surface area of crystal to volume of crystallizer ratio than those in the 0.6-L crystallizer, because the final mean crystal diameters of milk fat slurries from both scales were of the same order of magnitude. Thus, the scaled tip speed of a crystallizer (kinematic similarity) is not a true scale parameter for AMF fractionation.

Figure 3 shows the filtration data as a function of tip speed (calculated from Eq. 1). The data for the 0.6-L crystallizer showed the same optimum seen in Figure 2, but now the 3.6-L data followed the trend for the 0.6-L crystallizer more closely, indicating that tip speed may be a better scale-up parameter than scaled tip speed. Further investigation of mixing in the 3.6-L crystallizer and study of a third scale of fractionation is needed to verify that tip speed is a true scale-up parameter. However, care must be taken when using tip speed for scale-up, since it does not account for the size of the crystallizer. Settling in the 0.6-L crystallizer always occurred below a scaled tip speed of 0.50 s^{-1} since the agitator speed was too slow to suspend the crystals. Settling can occur at any tip speed given a large enough crystallizer because tip speed is not a function of the crystallizer diameter.

To determine the true scale criteria of a crystallization or mixing process, at least three different scales of operation must be studied. The surface heat transfer of both crystallizers was kept constant at 195 $kW \cdot m^{-2}$, but the different mixing speeds changed the rate of heat transfer through the milk fat for each operating condition. A possible scale parameter to study would then be constant heat transfer per unit volume of crystallizer. Other potential scale-up parameters that could be investigated with tip speed might include power number, mixing Reynolds number, Froude number and a constant solids suspension criteria characteristic for milk fat fractionation.

Crystal growth kinetics. Table 1 shows the results of fitting the growth curves, the mean size of the distribution changing with time, to Equation 3. The three parameters of Equation 3 relate to the final mean size (L_s), the predicted in-

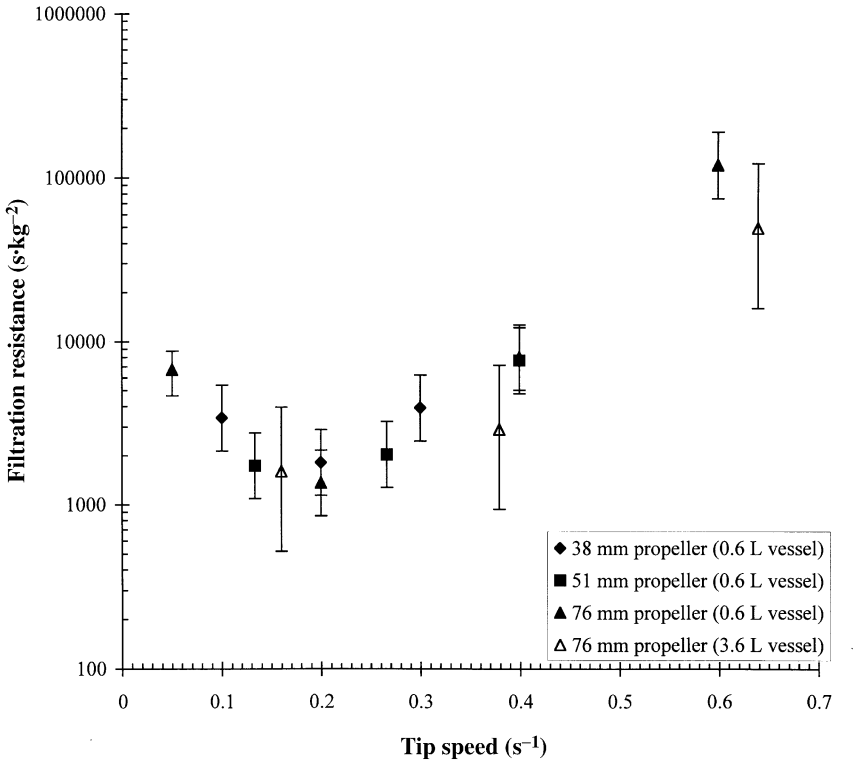

FIG. 3. Comparison of filtration resistances (Eq. 4) as a function of agitator tip speed of resultant slurries from batch crystallization of anhydrous milk fat (0.6 and 3.6 L, 28°C, 500 kPa). Error bars are 90% confidence intervals.

duction time for nucleation (L_D), and the time constant of crystallization (τ_C). Based on the variability of crystallization kinetics between experimental replicates, the confidence intervals of these parameters were relatively large. That is, sufficient variability in crystallization at the same operating conditions caused high uncertainty in the parameters estimated from the crystal growth data. Thus, no direct correlations between the crystallization parameters presented in Table 1 with either filtration rate data or physical properties of the solid fraction were observed. In the future, more careful nucleation and growth kinetics will be needed to fully understand the development of the crystal size distribution with time and how this affects filtration.

Properties of fractions. (i) Solid fraction yields. The yield of solid fat varied with agitator diameter and speed. Figure 4 shows the yield of the solid fraction as a function of the

TABLE 1
Summary of Crystal Growth Kinetic Curve Parameters from Equation 3[a]

#	Volume (L)	D (mm)	N (rpm)	L_s (μm)	t_c (min)	L_D (min)
1	0.6	38	50	180 ± 20	110 ± 30	60 ± 10
2	0.6	51	50	150 ± 10	90 ± 20	70 ± 10
3	0.6	76	50	150 ± 10	120 ± 30	40 ± 20
4	0.6	38	100	130 ± 10	90 ± 20	60 ± 10
5	0.6	51	100	110 ± 10	60 ± 20	60 ± 20
6	0.6	76	100	100 ± 5	40 ± 10	70 ± 10
7	0.6	38	150	110 ± 10	60 ± 20	60 ± 20
8	0.6	51	150	110 ± 5	70 ± 30	40 ± 30
9	0.6	76	150	90 ± 10	30 ± 20	50 ± 20
10	0.6	76	12.5	130 ± 10	170 ± 50	40 ± 30
11	3.6	76	40	180 ± 20	120 ± 60	70 ± 30
12	3.6	76	95	110 ± 10	80 ± 30	60 ± 20
13	3.6	76	160	100 ± 10	50 ± 40	50 ± 40

[a]D, impeller diameter; N, impeller speed; L_s, steady-state geometric mean equivalent crystal diameter ± 95% confidence interval; t_c, crystallizer time constant ± 95% confidence interval; L_D, predicted induction time for crystallization ± 95% confidence interval.

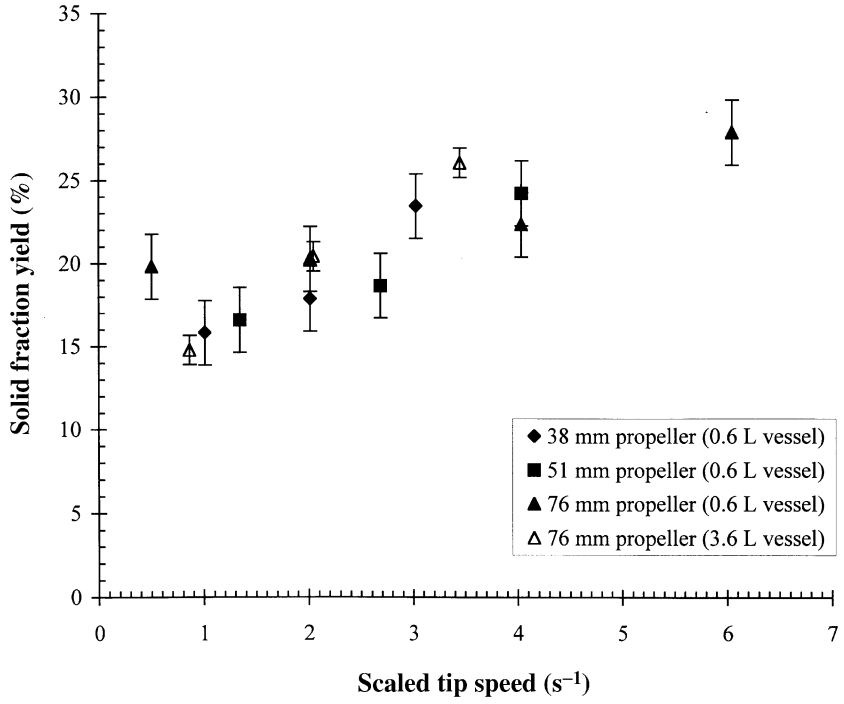

FIG. 4. Comparison of solid fraction yields after batch crystallization and pressure filtration of anhydrous milk fat (28°C, 500 kPa). Error bars are 90% confidence intervals.

scaled tip speed for both the 0.6- and 3.6-L crystallizers. This yield value also includes the mass of liquid oil entrained in the cake between and within milk fat crystals and agglomerates, which is a major problem associated with melt crystallization. The amount of entrained liquid in the cake varies with the experimental conditions. The solid fat yield generally increased with increasing scaled tip speed. The highest yield was measured for the 0.6-L crystallizer with the 76-mm propeller at an agitation speed of 150 rpm.

(ii) Filtration liquid entrainment. Figure 5 shows the amount of liquid entrainment (Equation 7) for pressure filtration at 500 kPa of the resultant milk fat slurries as calculated from the absorbance data. In general, as the scaled tip speed increased, the amount of liquid entrained in the cake increased and the efficiency of filtration decreased, although the variability in this measurement limited the statistical significance of these differences. There was an indication of minimal entrainment at u_{scaled} of 1.5 s^{-1}, although the difference in amount of entrained liquid at this scaled tip speed was not statistically significant. At a scaled tip speed of 6.0 s^{-1} (0.6-L crystallizer with the 76-mm propeller at an agitation speed of 150 rpm) the solid fraction contained 79% entrained liquid. The large number of small crystals formed at these conditions had a high crystal surface area to volume ratio, which allowed for more entrapment of liquid. Thus, the level of entrainment increased and filtration efficiency in the filter cake decreased (Fig. 3) compared to the filter cake produced at a scaled tip speed of 2.0 s^{-1} with 72% liquid entrained. The variation of the absorbance data between experiments created large confidence intervals for the filtration efficiency and entrainment calculation, making it difficult to conclude that an optimum existed, as seen previously. However, the trend for filtration efficiency to decrease and liquid entrainment to increase for scaled tip speed below 1.0 s^{-1} was apparent.

(iii) Melting (clear) points. Figure 6 shows the melting (clear) points of the solid fractions for all of the experiments in the 0.6- and 3.6-L crystallizers as a function of scaled tip speed. As for filtration rate (Fig. 2), the clear point also exhibited a maximum at a scaled tip speed of about 2.0 s^{-1}. The milk fat fraction produced at a scaled tip speed of 6.0 s^{-1} (0.6-L crystallizer with the 76-mm propeller at an agitation speed of 150 rpm) had a melting point of 42.2°C. Owing to liquid entrainment, this melting point was less than the melting point of 45.8°C of the milk fat fraction produced during crystallization at the optimal scaled tip speed of 2.0 s^{-1}. The milk fat fraction produced at a scaled tip speed of 0.5 s^{-1} (0.6-L crystallizer with the 76-mm propeller at an agitation speed of 12.5 rpm) had a melting point of 45.1°C. More liquid was entrained in this milk fat fraction because large agglomerates had formed during these experiments and liquid oil was entrained within the agglomerated network of fat crystals.

The melting (clear) points for milk fat fractions produced in the 3.6-L crystallizer did not follow the same trend. Again, the crystals produced in the 3.6-L crystallizer had a larger crystal surface area to crystallizer volume ratio and so collided less frequently with the crystallizer walls than in the 0.6-L crystallizer. Kinematic similarity or scaled tip speed was not a good scale-up parameter for milk fat fractionation.

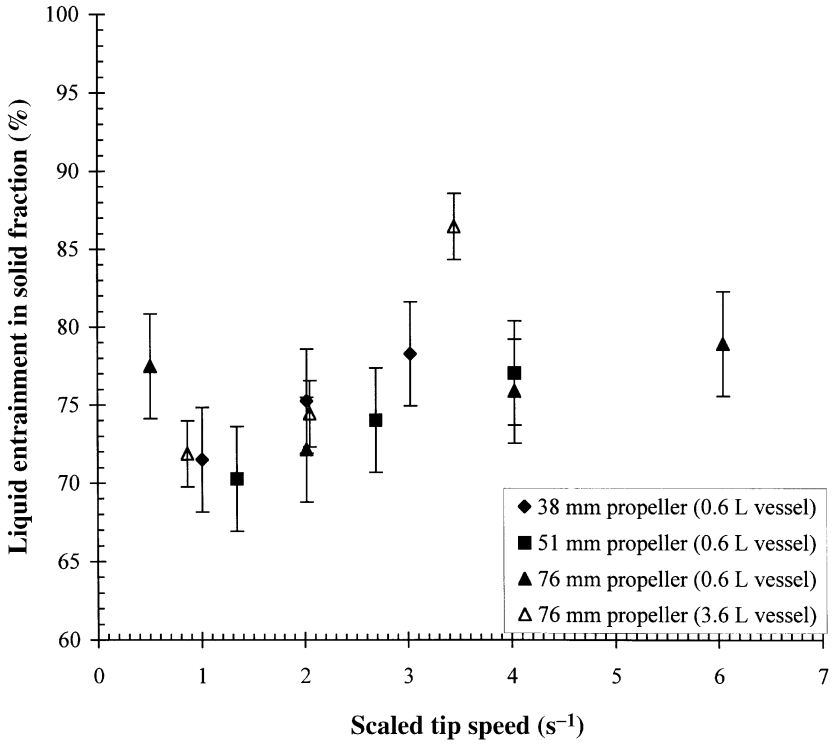

FIG. 5. Comparison of liquid entrainment (Eq. 7) in the solid fractions after batch crystallization and pressure filtration of anhydrous milk fat (28°C, 500 kPa). Error bars are 90% confidence intervals.

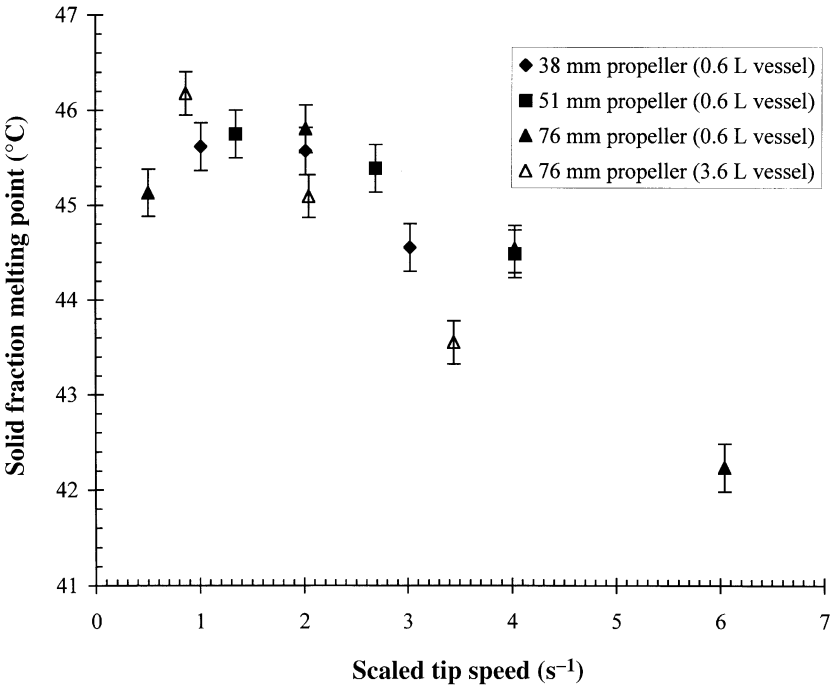

FIG. 6. Comparison of solid fraction melting clear points after batch crystallization and pressure filtration of anhydrous milk fat (28°C, 500 kPa). Error bars are 90% confidence intervals.

ACKNOWLEDGMENTS

This work was supported by the Wisconsin Milk Marketing Board and the New Zealand Dairy Board through the Wisconsin Center for Dairy Research. Special thanks to the milk fats research team at the New Zealand Dairy Research Institute.

REFERENCES

1. Jensen, R.G., A.M. Ferris, and C.J. Lammi-Keefe, The Composition of Milk Fat, *J. Dairy Sci. 74*:3228–3243 (1991).
2. Yoon, J., R.W. Hartel, and Y.C. Wang, Analysis of Butterfat Extraction and Fractionation Using Supercritical Carbon Dioxide, *J. Food Proc. Pres. 17*:471–484 (1993).
3. Arul, J., A. Boudreau, J. Makhlouf, R. Tardif, and M.R. Sahasrabudhe, Fractionation of Anhydrous Milk Fat by Supercritical Carbon Dioxide, *J. Food Sci., 52*:1231–1236 (1987).
4. Singh, B., and S.S.H. Rizvi, Design and Economic Analysis for Continuous Countercurrent Processing of Milk Fat with Supercritical Carbon Dioxide, *J. Dairy Sci. 77*:1731–1745 (1994).
5. Bhaskar, A.J., S.S.H. Rizvi, and P. Harriott, Performance of a Packed Column for Continuous Supercritical Carbon Dioxide Processing, *Biotechnol. Prog., 9*:70–74 (1993).
6. Arul, J., A. Boudreau, J. Makhlouf, R. Tardif, and T. Bellavia, Fractionation of Anhydrous Milk Fat by Short Path Distillation, *J. Am. Oil Chem. Soc. 65*:1642–1646 (1988).
7. Antila, V., The Fractionation of Milk Fat, *Milk Ind. 81*:17–20 (1979).
8. Badings, H.T., J.E. Schaap, C. de Jong, and H.G. Hagedoorn, An Analytical Study of Fractions Obtained by Stepwise Cooling of Melted Milk Fat. 2. Results, *Milchwissenschaft 38*:150–156 (1983).
9. Grall, D.S., and R.W. Hartel, Kinetics of Butterfat Crystallization, *J. Am. Oil Chem. Soc., 69*:741–747 (1992).
10. Larsen, N.E., and E.G. Samuelsson, Some Technological Aspects on Fractions of Anhydrous Butterfat, *Milchwissenschaft, 34*:663–665 (1979).
11. Amer, M.A., D.B. Kupranycz, and B.E. Baker, Physical and Chemical Characteristics of Butterfat Fractions Obtained by Crystallization from Molten Fat, *J. Am. Oil Chem. Soc. 62*: 1551–1557 (1985).
12. Deffense, E., Multi-Step Butteroil Fractionation and Spreadable Butter, *Fat Sci. Technol 89*:502–507 (1987).
13. Barna, C.M., R.W. Hartel, and S. Metin, Incorporation of Milkfat Fractions into Milk Chocolate, *Manufact. Confectioner 72*: 107–116 (1992).
14. Kaylegian, K.E., and R.C. Lindsay, Performance of Selected Milk Fat Fractions in Cold Spreadable Butter, *J. Dairy Sci. 75*:3307–3317 (1992).
15. Black, R.G., Partial Crystallization of Milkfat and Separation of Fractions by Vacuum Filtration, *Aust. J. Dairy Techol. 30*:153–156 (1975).
16. Black, R.G., Pilot Scale Studies of Milk Fat Fractionation, *Ibid. 28*:116–119 (1973).
17. Badings, H.T., J.E. Schaap, C. de Jong, and H.G. Hagedoorn, An Analytical Study of Fractions Obtained by Stepwise Cooling of Melted Milk Fat. 1. Methodology, *Milchwissenschaft, 38*:95–97 (1983).
18. Deffense, E., Milk Fat Fractionation Today: A Review, *J. Am. Oil Chem. Soc. 70*:1193–1201 (1993).
19. Breeding, C.J., and R.T. Marshall, Crystallization of Butteroil and Separation by Filter Centrifugation, *Ibid. 72*:449–453 (1995).
20. Evans, A.A., Colour Measurements in Milk Fat Fractionation, *NZ J. Dairy Sci. Technol. 11*:73–78 (1976).
21. Kaylegian, K.E., R.W. Hartel, and R.C. Lindsay, Applications of Modified Milk Fat in Food, *J. Dairy Sci. 76*:1782–1796 (1993).
22. Timms, R.E., The Phase Behavior of Mixtures of Milk Fat and Cocoa Butter, *Lebensm. Wiss. Technol. 13*:61–65 (1980).
23. Timms, R.E., and J.V. Parekh, The Possibilities for Using Hydrogenated, Fractionated or Interesterified Milk Fat in Chocolate, *Ibid. 13*:177–181 (1980).
24. Lohman, M., and R.W. Hartel, Effect of Milk Fat Fractions on Fat Bloom in Dark Chocolates, *J. Am. Oil Chem. Soc. 71*:267–276 (1994).
25. Hartel, R.W., Application of Milk Fat Fractions in Confectionery, *Ibid. 73*:945–953 (1996).
26. Kaylegian, K.E., and R.C. Lindsay, *Handbook of Milkfat Fractionation Technology and Applications*, AOCS Press, Champaign, 1995.
27. Box, G.E.P., W.G. Hunter, and J.S. Hunter, *Statistics for Experimenters*, John Wiley & Sons, New York, 1978, pp. 208–228.
28. McCabe, W.L., J.C. Smith, and P. Harriott, *Unit Operations of Chemical Engineering*, 4th edn., McGraw-Hill Book Company, New York, 1985, pp. 217, 871–878.
29. Schaap, J.E., and G.A.M. Rutten, Colorimetric Method, Based on the Carotene Content, for the Estimation of the Percentage of Solids in Butterfat with Crystals, *Neth. Milk Dairy J. 28*:166–174 (1974).
30. *Official Methods and Recommended Practices of the American Oil Chemists' Society*, 4th edn., American Oil Chemists' Society, Champaign, 1989, Method Cc 1–25.

[Received November 30, 1998; accepted February 24, 1999]